Time-delay high-order sliding mode control for trajectory tracking of autonomous underwater vehicles under disturbances

Jesus Guerrero, Ahmed Chemori, Jorge Torres, Vincent Creuze

Time-delay high-order sliding mode control for trajectory tracking of autonomous underwater vehicles under disturbances

Jesus Guerrero[a], Ahmed Chemori[b,*], Jorge Torres[c] and Vincent Creuze[b]

[a]*Tecnologico Nacional de Mexico/ ITS Abasolo, Guanajuato, Mexico*
[b]*LIRMM, University of Montpellier, CNRS, Montpellier, France*
[c]*Center for Research and Advanced Studies of the National Polytechnic Institute (CINVESTAV), Mexico City, Mexico.*

ARTICLE INFO

ABSTRACT

This paper presents a new generalized super-twisting algorithm (GSTA) controller with a time-delay estimator (TDE) for the tracking control of an autonomous underwater vehicle (AUV) under disturbances. For exploration tasks in confined areas, AUVs are typically equipped with sensors such as Doppler velocity logs (DVL) or acoustic modems to measure their position and speed. However, these sensors have a disadvantage in that their acquisition rates are low. This disadvantage, combined with the influence of external disturbances, directly influences position control because it requires partial knowledge of the system for proper operation. To solve this problem, the introduction of a TDE that estimates the vehicle hydrodynamics with delayed sensor information, and consequently, improves the controller performance is proposed. For controller validation, a stability analysis is presented, and two results are provided in the simulation. In the first test, the AUV is controlled to track a parameterized spiral-shaped path to validate the vehicle movement in the three directions of the plane (x, y, z). In the second test, the AUV performs path tracking in yaw and depth motions. In all numerical simulations, three types of disturbances/uncertainties are considered: (i) system parameters, (ii) sensor readings, and (iii) control.

1. Introduction and related work

Autonomous underwater vehicles (AUVs) have become popular in recent years owing to their wide range of application in military, commercial, and scientific fields. Indeed, numerous scanning and monitoring tasks are today performed in deep water, where intrinsic human limitations do not allow access. Therefore, AUVs have positioned themselves as an acceptable choice for this type of task.

To perform tasks efficiently, AUVs require a degree of autonomy; for example, to position the vehicle at a specific pose or to track a path for mapping an area of interest. Accordingly, the control of AUVs is one of the most challenging requirements in performing any task. Therefore, in recent years, different control techniques have been proposed.

Linear controllers for AUVs are based on PD/PIDs Jalving (1994); Busquets et al. (2012); Fossen (1994) and their variants Smallwood and Whitcomb (2004); Rathore and Kumar (2015a). These are simple to implement yet lack robustness against external disturbances Tabar et al. (2015), even though nonlinear variants have been proposed Guerrero et al. (2020b, 2019b). Robust controllers have also been proposed, including sliding mode controllers (SMC) Salgado-Jimenez and Jouvencel (2003); Elmokadem et al. (2016), fuzzy techniques Kanakakis et al. (2004), neuronal approaches Amin et al. (2010), adaptive techniques Huang et al. (2013, 2014); Tijjani et al. (2020); Guerrero et al. (2020a); Maalouf et al.

(2012); Guerrero et al. (2019a), global stable tracking control with input saturation Huang et al. (2015); Campos et al. (2017); Guerrero et al. (2019b); Campos et al. (2019), backstepping control Guerrero et al. (2018), predictive control Shen et al. (2018), and adaptive variations Li and Lee (2005); Chen et al. (2016); Rezazadegan et al. (2015). For a detailed review of the literature on AUV control, please refer to Tijjani et al. (2022). Sliding mode control (SMC) is a popular and robust technique used in several fields including marine robotics. This technique provides finite-time convergence and robustness against parametric uncertainties and matched external disturbances. In its basic implementation (first-order SMC), this controller can exhibit aggressive control input behavior (chattering phenomenon) owing to the signum function, which can damage the system's actuators. This negative effect appears during the reaching condition and tends to be sensitive to inaccurate mathematical models. The classical approaches to chattering attenuation in SMC systems are as follows.

(i) Partial knowledge of the system's parameters. Under the SMC technique, the controller is typically divided into two terms: the nominal part, which compensates and cancels the nonlinearities of the model through a partial knowledge of the system, and the weighted switching function, which is responsible for canceling the effect of the external disturbances. As expected, if the system's model parameters are known, the gain of the switch function can be maintained at a small value, which reduces the chattering amplitude. If only minimum information regarding the parameters is available, the gain must be increased to compensate for the

*Corresponding author

✉ jguerrero@abasolo.tecnm.mx (J. Guerrero);
Ahmed.Chemori@lirmm.fr (A. Chemori); jtorres@ctrl.cinvestav.mx (J. Torres); vincent.creuze@lirmm.fr (V. Creuze)
ORCID(s):

modeling errors and disturbance effects. However, the amplitude of the chattering is also increased.

(ii) Replacing the discontinuous control function by saturation or sigmoid functions. This action smooths the control signal. However, this is at the cost of loss of robustness because it constrains the sliding system's trajectories to the sliding surface vicinity Shtessel et al. (2014).

(iii) Adopting a high-order sliding mode control (HOSMC) approach. This methodology exploits quasi-continuous control, which allows driving to the origin the sliding surface and its derivative in the presence of matched external disturbances.

Furthermore, it is well known that the sliding mode technique is sensitive to large time delays in a controlled system, which can degrade controller performance Utkin et al. (2017); Fridman et al. (1996); Gouaisbaut et al. (2002). In underwater vehicles, sensors can induce large delays. Consider, for example, the case of the Doppler velocity log (DVL), which is used to measure the ground speed of a vehicle based on acoustic measurements. This time delay must be considered in the control design to minimize its negative effect on the closed-loop performance.

In this study, we propose the design of a robust controller that considers these issues. On one hand, the large time delays induced by the sensors or the communication system are considered. However, we also assume that some of the hydrodynamic parameters of the AUV are unknown. The proposed controller is based primarily on two techniques. The first is the generalized super twisting algorithm (GSTA) Moreno (2009), which is the generalization of the classical super-twisting (STW) controller introduced by Levant Levant (1993). This controller includes a linear version of the algorithm, standard STW, and STW with extra linear correction terms that provide more robustness and convergence velocity. It is noteworthy that this method continues to require partial information regarding the parameters of the system. The second is the time-delay estimator (TDE) that estimates the hydrodynamic parameters of underwater vehicles. This methodology was introduced initially in Hsia (1989) to estimate certain parameters and disturbances in the model using the time-delayed information of the state derivatives and input control. Furthermore, this method considers the time delay induced by sensors when estimating the parameters. TDE has been employed in the field of mobile robotics for the control of robotic manipulator arms, where certain parameters are difficult to estimate Hsia et al. (1991a); Jin et al. (2008). Later, this method was introduced in the field of underwater vehicles as an option for estimating the hydrodynamic parameters Kim et al. (2016).

This study introduces an approach that is different from that proposed in Kim et al. (2016). The main contributions of this study can be summarized as follows:

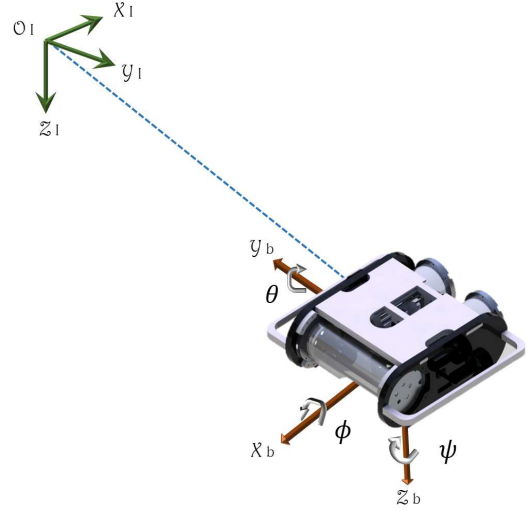1. The robust trajectory tracking problem is considered.

Figure 1: Illustration of vehicle's reference frames. The inertial fixed frame is denoted (O_I, X_I, Y_I, Z_I); the body-fixed frame is denoted (O_b, X_b, Y_b, Z_b).

2. The assumption of having decoupled yaw motion from surge and sway motions, which could be restrictive when considering trajectory-tracking problems is avoided.

3. TDE estimates the AUV parameters through the time-delayed information of the available states and control input only. Then, these parameters are inserted into the GSTA control law to maintain the gains at a low value to reduce the chattering amplitude. Note that information a priori regarding the parameters of the system is not required.

4. The closed-loop stability of the GSTA controller with TDE estimator is analyzed by Lyapunov arguments, such that practical stability can be concluded.

The remainder of this paper is organized as follows. In Section 2, the dynamic model of the AUV is introduced. In Section 3, the proposed controller based on GSTA and TDE is detailed. Section 4 is devoted to closed-loop stability analysis based on Lyapunov arguments while considering disturbances and non-modeled hydrodynamics. The numerical simulation results for tracking the three-dimensional (3D) trajectories are provided in Section 5. Finally, Section 6 presents the conclusions and future work.

2. Dynamic model of the vehicle

Dynamic models of underwater vehicles have been described in several studies Fossen (1994); Fossen; Prestero (2001); Kinsey et al. (2006). First, let us consider the mathematical model of a marine vehicle given by

$$M\dot{v} + C(v)v + D(v)v + g(\eta) = \tau, \qquad (1)$$
$$\dot{\eta} = J(\eta)v, \qquad (2)$$

where $v = [u, v, w, p, q, r]^T$ is the state vector of the velocity relative to the body-fixed frame and $\eta = [x, y, z, \phi, \theta, \psi]^T$ represents the vector of the position and orientation relative to the inertial frame (see Figure 1). $M \in \mathbb{R}^{6 \times 6}$ is the matrix of inertia, where the effects of added mass are included; $C(v) \in \mathbb{R}^{6 \times 6}$ is the Coriolis-centripetal matrix; $D(v) \in \mathbb{R}^{6 \times 6}$ represents the hydrodynamic damping matrix; $g(\eta) \in \mathbb{R}^6$ is the vector of gravitational and buoyancy forces and moments. Finally, $\tau \in \mathbb{R}^6$ is the control vector acting on the underwater vehicle and $J(\eta) \in \mathbb{R}^{6 \times 6}$ is the transformation matrix mapping from the body-fixed frame to the earth-fixed frame.

In our study, we assume that the AUV is designed to be intrinsically stable in roll and pitch Salgado-Jiménez et al. (2011); Rathore and Kumar (2015b); Caccia and Veruggio (2000). This assumption is exploited to simplify the model of the vehicle and reduce its dynamics to only four degrees of freedom, given by

$$m_u(t)\dot{u}(t) = m_v(t)v(t)r(t) - k_u u(t) - k_{u|u|}u(t)|u(t)|$$
$$+ F_u(t) + \rho_u(t), \quad (3)$$
$$m_v(t)\dot{v}(t) = -m_u(t)u(t)r(t) - k_v v(t) - k_{v|v|}v(t)|v(t)|$$
$$+ F_v(t) + \rho_v(t), \quad (4)$$
$$m_w(t)\dot{w}(t) = -k_w w(t) - k_{w|w|}w(t)|w(t)|$$
$$+ F_w(t) + W(t) + \rho_w(t), \quad (5)$$
$$I_r(t)\dot{r}(t) = -(m_v(t) - m_u(t))u(t)v(t) - k_r r(t)$$
$$- k_{r|r|}r(t)|r(t)| + T_r(t) + \rho_r(t), \quad (6)$$

where the surge (u), sway (v), and heave (w) are the translational speeds along O_{xb}, O_{yb}, O_{zb}, respectively. The yaw (r) is the rotational velocity along the z-axis, $m_u(t)$, $m_v(t)$, $m_w(t)$, and I_r are the vehicle mass and moment of inertia (including added mass and inertia). The terms $F_u(t)$, $F_v(t)$, and $F_w(t)$ represent the forces applied by the thrusters along the surge, sway, and heave directions, respectively. T_r is the torque on the yaw motion and $W(t)$ is the buoyancy force on the heave. Note that hydrodynamic damping is modeled as a linear and quadratic term, and $k_u \backslash k_{u|u|}$, $k_v \backslash k_{v|v|}$, $k_w \backslash k_{w|w|}$, and $k_r \backslash k_{r|r|}$ are the linear and quadratic damping coefficients in surge, sway, heave, and yaw, respectively. Finally, $\rho_u(t)$, $\rho_v(t)$, $\rho_w(t)$, and $\rho_r(t)$ are bounded disturbances along each direction.

Under the assumption that the vehicle is intrinsically stable in pitch and roll, the transformation matrix $J(\eta)$ in (2) is simplified, and the vehicle kinematics modeled as follows:

$$\dot{x}(t) = u(t)cos(\psi(t)) - v(t)sin(\psi(t)), \quad (7)$$
$$\dot{y}(t) = u(t)sin(\psi(t)) + v(t)cos(\psi(t)), \quad (8)$$
$$\dot{z}(t) = w(t), \quad (9)$$
$$\dot{\psi}(t) = r(t). \quad (10)$$

In Kim et al. (2016), yaw dynamics were not considered in the controller design procedure. In this approach, yaw dynamics are considered for the trajectory tracking controller design. Now, let us consider $\xi_1(t) = [x(t), y(t), z(t), \psi(t)]^T$

and $\xi_2(t) = [u(t), v(t), w(t), r(t)]^T$. Then, the set of nonlinear differential equations (3)–(10) can be rewritten as follows:

$$\dot{\xi}_1(t) = J(\psi)\xi_2(t), \quad (11)$$
$$M\dot{\xi}_2(t) = G(\xi) + F_\tau(t) + \Omega(t), \quad (12)$$

where the mass matrix is defined as $M = diag\{m_u(t), m_v(t), m_w(t), I_r(t)\}$ and the control inputs are synthesized in vector form as $F_\tau(t) = [F_u(t), F_v(t), F_w(t), T_r(t)]^T$. The vector of the external disturbances is defined as $\Omega(t) = [\rho_u(t), \rho_v(t), \rho_w(t), \rho_r(t)]^T$. Finally, the matrices $J(\psi)$ and $G(\xi)$ are given by

$$J(\psi) = \begin{bmatrix} cos(\psi) & -sin(\psi) & 0 & 0 \\ sin(\psi) & cos(\psi) & 0 & 0 \\ 0 & 0 & 1 & 0 \\ 0 & 0 & 0 & 1 \end{bmatrix}, \quad (13)$$

$$G(\xi) = \begin{bmatrix} g_u(t) \\ g_v(t) \\ g_w(t) \\ g_r(t) \end{bmatrix}, \quad (14)$$

with

$$g_u(t) = m_v(t)v(t)r(t) - k_u u(t) - k_{u|u|}u(t)|u(t), | \quad (15)$$
$$g_v(t) = -m_u(t)u(t)r(t) - k_v v(t) - k_{v|v|}v(t)|v(t), | \quad (16)$$
$$g_w(t) = -k_w w(t) - k_{w|w|}w(t)|w(t), | \quad (17)$$
$$g_r(t) = -(m_v(t) - m_u(t))u(t)v(t) - k_r r(t) - \quad (18)$$
$$- k_{r|r|}r(t)|r(t).| \quad (19)$$

3. Proposed control design

In this section, the design of two robust controllers for trajectory tracking of an underwater vehicle is proposed. First, based on the assumption that the hydrodynamic parameters of the vehicle are unknown, the construction of the GSTA nominal design is presented. In the second step, the TDE approach is adapted to the underwater vehicle system to estimate the unknown dynamics using information stored in the central computer of the vehicle. Then, the estimation made by the TDE method is introduced into the previous controller nominal design to enhance it.

3.1. GSTA nominal design

First, model (11)âĂŞ-(12) must be expressed in a proper form. Therefore, the following state variables are chosen:

$$\begin{bmatrix} \zeta_1(t) \\ \zeta_2(t) \end{bmatrix} = \begin{bmatrix} \xi_1(t) \\ \dot{\xi}_1(t) \end{bmatrix}. \quad (20)$$

Then, from Equation (11), we obtain the following useful algebraic relations:

$$\xi_2(t) = J(\psi)^{-1}\dot{\xi}_1(t), \quad (21)$$
$$\dot{\xi}_2(t) = J(\psi)^{-1}\ddot{\xi}_1(t) - J(\psi)^{-1}\dot{J}(\psi)J(\psi)^{-1}\dot{\xi}_1(t). \quad (22)$$

Finally, using the relations stated above, system (11)âĂŞ-(12) can be rewritten as follows:

$$\dot{\zeta}_1(t) = \zeta_2(t), \tag{23}$$

$$\dot{\zeta}_2(t) = \pi_1(\zeta) + \pi_2(\zeta) + \gamma_1(\zeta)F_\tau(t) + \overline{\Omega}(t), \tag{24}$$

where the vectors $\pi_1(\zeta)$ and $\pi_2(\zeta)$, and matrix $\gamma_1(\zeta)$ are given by

$$\pi_1(\zeta) = \dot{J}(\psi)J(\psi)^{-1}\zeta_2(t), \tag{25}$$

$$\pi_2(\zeta) = J(\psi)M^{-1}G(\xi_1, \xi_2), \tag{26}$$

$$\gamma_1(\zeta) = J(\psi)M^{-1}, \tag{27}$$

$$\overline{\Omega}(t) = J(\psi)M^{-1}\Omega(t). \tag{28}$$

The next step is to design the controller to enforce the sliding mode on the manifold.

$$\sigma(t) = \dot{e}(t) + \Gamma e(t), \tag{29}$$

where the sliding surface is defined as $\sigma(t) = [\sigma_1(t), \sigma_2(t), \sigma_3(t), \sigma_4(t)]^T$. The tracking error and its time derivative are defined as $e = \zeta_1^d(t) - \zeta_1(t)$ and $\dot{e} = \dot{\zeta}_1^d(t) - \zeta_2$, respectively, where $\zeta_1^d(t) = [x_d(t), y_d(t), z_d(t), \psi_d(t)]^T$ is the desired trajectory, and $\dot{\zeta}_1^d(t)$ represents the time derivative of the desired trajectory. $\Gamma = diag(\Gamma_1, \Gamma_2, \Gamma_3, \Gamma_4)$ denotes a definite positive matrix. Before proposing the control law, it is necessary to make the following assumption. *Assumption 1.* The perturbation $\overline{\Omega}(t)$ is a Lipschitz continuous function and its time derivative is bounded by

$$|\dot{\overline{\Omega}}_i(t)| \le L_i|\phi_2(\sigma)|, \qquad i = \overline{1,4}, \tag{30}$$

where $L_i \ge 0$ is a finite unknown boundary. In this study, we assume that the waves and currents satisfy Assumption 1. The control law based on the sliding-mode controller is given by

$$F_\tau(t) = \gamma_1(\zeta)^{-1}\left[\ddot{\zeta}_1^d(t) + \Gamma\dot{e} - \pi_1(\zeta) - \pi_2(\zeta) - \vartheta\right], \tag{31}$$

where the GSTA ϑ is defined as follows:

$$\begin{aligned}\vartheta &= -K_1\Phi_1(\sigma) + \lambda \\ \dot{\lambda} &= -K_2\Phi_2(\sigma),\end{aligned} \tag{32}$$

where $\Phi_1(\sigma) = [\phi_{11}, \phi_{12}, \phi_{13}, \phi_{14}]^T$ and $\Phi_2(\sigma) = [\phi_{21}, \phi_{22}, \phi_{23}, \phi_{24}]^T$, each element of which is given by

$$\begin{aligned}\phi_{1i}(\sigma_i) &= \mu_{1i}|\sigma_i|^{1/2}sgn(\sigma_i) + \mu_{2i}\sigma_i, \\ \phi_{2i}(\sigma_i) &= \frac{1}{2}\mu_{1i}^2 sgn(\sigma_i) + \frac{3}{2}\mu_{1i}\mu_{2i}|\sigma_i|^{1/2}sgn(\sigma_i) + \mu_{2i}^2\sigma_i,\end{aligned} \tag{33}$$

where $\mu_{1i}, \mu_{2i} \ge 0$ with $i = \overline{1,4}$, and $sgn(\star)$ is the signum function, defined as

$$sgn(\star) = \begin{cases} 1 & \text{if } \star > 0 \\ -1 & \text{if } \star < 0 \\ \alpha, \quad \alpha \in [-1,1] & \text{if } \star = 0, \end{cases} \tag{34}$$

where α is scalar. The gain matrices are diagonal and positive definite, that is, $K_1 = diag\{k_{11}, k_{12}, k_{13}, k_{14}\}$ and $K_2 = diag\{k_{21}, k_{22}, k_{23}, k_{24}\}$.

Finally, assume that information regarding the underwater vehicle hydrodynamic parameters are not available, meaning $G(t)$ is unknown. Then, in (31), the term $\pi_2(\xi)$ is not considered and the controller can be rewritten as follows:

$$F_\tau(t) = \gamma_1(\zeta)^{-1}\left[\ddot{\zeta}_1^d(t) + \Gamma\dot{e} - \pi_1(\zeta) - \vartheta\right]. \tag{35}$$

3.2. GSTA design with TDE

In this section, to overcome the lack of information regarding the hydrodynamic parameters of the AUV, the proposed controller, based on the GSTA, is improved by introducing the TDE into the final control law expression. As mentioned above, the procedure is divided into three main steps, detailed in the following.

Step 1. Before proceeding to express the AUV model in a proper form, which allows us to obtain the SMC, it is necessary to introduce certain modifications. First, following the procedure used by Jin et al. (2008), we introduce the matrix defined as $\overline{M} = diag(\overline{m}_u, \overline{m}_v, \overline{m}_w, \overline{I}_r)$, which contains the control parameters $\overline{m}_u, \overline{m}_v, \overline{m}_w$, and $\overline{I}_r$ into (12). Then, Equations (11) and (12) can be rewritten as follows:

$$\dot{\xi}_1(t) = J(\psi)\xi_2(t), \tag{36}$$

$$\overline{M}\dot{\xi}_2(t) + H(t) = F_\tau(t), \tag{37}$$

where the elements of $H(t) = [h_u(t), h_v(t), h_w(t), h_r(t)]^T$ are defined as follows:

$$\begin{aligned}h_u(t) &= (m_u(t) - \overline{m}_u)\dot{u}(t) + k_u u(t) + k_{u|u|}u(t)|u(t)|, \\ &\quad - m_v(t)v(t)r(t) - \rho_u(t), \\ .h_v(t) &= (m_v(t) - \overline{m}_v)\dot{v}(t) + k_v v(t) + k_{v|v|}v(t)|v(t)|, \\ &\quad + m_u(t)u(t)r(t) - \rho_v(t), \\ .h_w(t) &= (m_w(t) - \overline{m}_w)\dot{w}(t) + k_w w(t) + k_{w|w|}w(t)|w(t)|, \\ &\quad - W(t) - \rho_w(t). \\ h_r(t) &= (I_r(t) - \overline{I}_r)\dot{r}(t) + k_r r(t) - k_{r|r|}r(t)|r(t)| \\ &\quad + (m_v(t) - m_u(t))u(t)v(t) - \rho_r(t).\end{aligned}$$

By choosing the same state variables given by Equation (20) and introducing Equations (21) and (22) into (37), the dynamic system (36)–(37) can be represented as follows:

$$\dot{\zeta}_1(t) = \zeta_2(t), \tag{38}$$

$$\dot{\zeta}_2(t) = \pi_1(\zeta) + \pi_3(\zeta) + \gamma_2(\zeta)F_\tau(t), \tag{39}$$

where the function $\pi_1(\zeta)$ is defined by (25), and the vector $\pi_3(\zeta)$ and matrix $\gamma_2(\zeta)$ are given by

$$\pi_3(\zeta) = J(\psi)\overline{M}^{-1}H(t), \tag{40}$$

$$\gamma_2(\zeta) = J(\psi)\overline{M}^{-1}. \tag{41}$$

Step 2. As in the nominal case stated earlier, it is necessary to introduce the following assumption.

Assumption 2. The TDE error is defined as

$$\epsilon(t) = J(\psi)\overline{M}^{-1}[H(t) - \Delta\hat{H}(t),] \tag{42}$$

where its derivative is considered to be bounded. The proof is given by Jin et al. (2008) and Hsia et al. (1991b), and adapted to the AUV paradigm by Kim et al. (2016).

Employing the same sliding surface given by Equation (29), the sliding mode controller is constructed as follows:

$$F_\tau(t) = \gamma_2(\zeta)^{-1}\left[\ddot{\xi}_1^d(t) + \Gamma\dot{e} - \pi_1(\zeta) - \pi_3(\zeta) - \vartheta\right], \tag{43}$$

where the GSTA ϑ is defined in Equations (32) and (33).

Step 3. It is noteworthy that for the control law presented by (43), the exact knowledge of $\pi_1(\zeta)$ and $\pi_3(\zeta)$ is necessary. The DVL provides information regarding the position of the AUV, which means that the term $\pi_1(\zeta)$ is known. However, term $\pi_3(\zeta)$, which is directly related to the underwater vehicle model, is unknown. Thus, the controller given by (43) is not feasible. To overcome this restriction, we propose using the TDE to estimate $H(t)$ from (40).

In this sense, an efficient engineering solution to estimate the function $H(t)$ is brought closer through its delayed function $H(t - h)$, where h is the given delay Hsia et al. (1991b). By defining the estimated matrix as $\hat{H}(t)$, from (37), we obtain the following:

$$\hat{H}(t) = H(t - h) = F_\tau(t - h) - \overline{M}\dot{\xi}_2(t - h). \tag{44}$$

This method is known as TDE. It is simple to implement because it only requires information stored in the central computer. However, there is a trade-off between the proposed method and error $\tilde{H}(t) = H(t) - \hat{H}(t)$, which increases as h increases Jung et al. (2004). This is related to the sampling frequency of the sensors; that is, if the sampling frequency is low, the error tends to increase.

For AUV localization in the $(x - y)$ plane, a DVL sensor or acoustic modem is used, which has a sampling frequency of approximately 3 to 5 Hz. This sampling time is considerably greater than that of other sensors such as an IMU or pressure sensor. Therefore, the TDE error increases, as stated above. To minimize this error, in Kim et al. (2016), a PD + SMC action with a weighted TDE term $\Delta\hat{H}(t)$ was considered. In this work, we extend the analysis to include a high-order sliding mode controller, namely GSTA, which decreases the convergence in finite time and softens the control action, as discussed below.

Therefore, the estimated term $\hat{H}(t)$ provided by Equation (44) is inserted into control law (43), leading to

$$F_\tau(t) = \overline{M}J(\psi)^{-1}\left[\ddot{\xi}_1^d(t) + \Gamma\dot{e} - \pi_1(\zeta) - \vartheta\right] - \Delta\hat{H}(t), \tag{45}$$

where $\Delta = diag\{\Delta_1, \Delta_2, \Delta_3, \Delta_4\}$ is an adjustable and positive-gain matrix. Moreover, the control law (45) can be rewritten using relations (44) and (22) to obtain the following controller in terms of the available variables:

$$F_\tau(t) = \overline{M}J(\psi)^{-1}\left[\ddot{\xi}_1^d(t) + \Gamma\dot{e} - \dot{J}(\psi)J(\psi)^{-1}\zeta_2(t) - \vartheta\right]$$

$$- \Delta\Big[F_\tau(t - h) - \overline{M}[J(\psi)^{-1}\dot{\zeta}_2(t - h) -$$

$$- J(\psi)^{-1}\dot{J}(\psi)J(\psi)^{-1}\zeta_2(t - h)]\Big]. \tag{46}$$

Finally, if the gains are selected as $K_1, K_2 > 0$ and are sufficiently large, it can be concluded that $\dot{\sigma}(t) \to 0$ in finite time, and based on equation (29), $\lim_{t\to\infty} e = 0$ and $\lim_{t\to\infty} \dot{e} = 0$.

The proof of the finite-time convergence of variables $\zeta_1(t)$ and $\zeta_2(t)$ into a small neighborhood of the desired reference signals $\zeta_1^d(t)$ and $\zeta_2^d(t)$ is given as follows.

Remark 1. *When the control objective is achieved, $\dot{\sigma}(t) \to 0$ and then $\sigma(t) \to 0$. Using Equation (29), one can note that $e(t) \to 0$ in finite time. Besides, the tracking error is defined as $e(t) = \zeta_1^d(t) - \zeta_1(t)$, and when the error approaches zero, it is implied that $\zeta_1(t) \to \zeta_1^d(t)$ in finite time.*

Remark 2. *The controller law developed in Equation (31) coincides with the law developed in the study of Guerrero et al. (2018). Moreover, following the assumption that information regarding the dynamic model of the underwater vehicle is not available, we modified the controller as indicated in Equation (35), where the term π_2, which is related to the hydrodynamic parameters, was suppressed. In our approach, as only information from the sensors is provided, we applied the TDE to estimate the hydrodynamic parameters, as we can see in the proposed control law (46), which depends only on the available information.*

4. Stability analysis

To formalize the stability analysis of robust path tracking based on sliding mode control theory, we introduce the following theorem:

Theorem 1. *Consider system (38)-(39) and GSTA (32) with perturbation terms. Suppose that the perturbation terms of system (56) are bounded. Then, gains K_1 and K_2 can be selected to be sufficiently high such that the error trajectories satisfy the strong practical stability notion, i.e., the error trajectories $e(t) = \zeta_1^d(t) - \zeta_1(t)$ are bounded and converge in finite time to the origin.*

Proof. From the derivative of (29) and substituting (45) and (32) into (39), one obtains the closed-loop dynamics given by

$$\dot{\sigma} = -K_1\left[\mu_{1i}|\sigma_i|^{\frac{1}{2}}sgn(\sigma_i) + \mu_{2i}\sigma_i\right]$$

$$- K_2\int_0^t\left[\frac{1}{2}\mu_{1i}^2 sgn(\sigma_i(\tau)) + \frac{3}{2}\mu_{1i}\mu_{2i}|\sigma_i(\tau)|^{\frac{1}{2}}sgn(\sigma_i(\tau))\right.$$

$$\left. + \mu_{2i}^2\sigma_i(\tau)\right]d\tau + J(\psi)\overline{M}^{-1}\left[H(t) - \Delta\hat{H}(t)\right]. \tag{47}$$

Then, considering Assumption 2, Equation (47) can be rewritten as follows:

$$\dot{\sigma} = -K_1\Phi_1(\sigma) - K_2\int_0^t\Phi_2(\tau)d\tau + \epsilon(t). \tag{48}$$

The equation above can be rewritten in an explicit form as

$$\dot{\sigma} = -K_1 \left[\mu_{1i} |\sigma_i|^{\frac{1}{2}} sgn(\sigma_i) + \mu_{2i} \sigma_i \right] + \epsilon(t)$$
$$- K_2 \int_0^t \left[\frac{1}{2} \mu_{1i}^2 sgn(\sigma_i(\tau)) + \frac{3}{2} \mu_{1i} \mu_{2i} |\sigma_i(\tau)|^{\frac{1}{2}} sgn(\sigma_i(\tau)) \right.$$
$$\left. + \mu_{2i}^2 \sigma_i(\tau) \right] d\tau. \tag{49}$$

Remark 3. *Note that* (47) *and* (49) *clearly indicate the influence of TDE error on the σ dynamics, i.e., $\epsilon(t)$ causes the resulting dynamics to deviate from the $\sigma(t)$ dynamics. Therefore, in this proof, $\epsilon(t)$ is considered a disturbance term. This result corroborates the conclusions of Jin et al. (2008) and Kim et al. (2016):*

Now, let:

$$s_{1i} = \sigma_i, \tag{50}$$
$$s_{2i} = -k_{2i} \int_0^t \phi_{2i}(\sigma_i(\tau)) d\tau + \epsilon_i(t), \tag{51}$$
$$\dot{\epsilon}_i(t) = \beta_i(t). \tag{52}$$

Then, Equation (49) can be rewritten in scalar form (for $i = \overline{1, 4}$) as follows:

$$\dot{s}_{1i} = -k_{1i} \left[\mu_{1i} |s_{1i}|^{\frac{1}{2}} sgn(s_{1i}) + \mu_{2i} s_{1i} \right] + s_{2i}, \tag{53}$$
$$\dot{s}_{2i} = -k_{2i} \left[\frac{1}{2} \mu_{1i}^2 sgn(s_{1i}) + \frac{3}{2} \mu_{1i} \mu_{2i} |s_{1i}|^{\frac{1}{2}} sgn(s_{1i}) + \right.$$
$$\left. + \mu_{2i}^2 s_{1i} \right] + \beta_i. \tag{54}$$

Without loss of generality, we can represent the system with simplified notation as follows:

$$\dot{s}_1 = -k_1 \left[\mu_1 |s_1|^{\frac{1}{2}} sgn(s_1) + \mu_2 s_1 \right] + s_2, \tag{55}$$
$$\dot{s}_2 = -k_2 \left[\frac{1}{2} \mu_1^2 sgn(s_1) + \frac{3}{2} \mu_1 \mu_2 |s_1|^{\frac{1}{2}} sgn(s_1) + \mu_2^2 s_1 \right] + \beta. \tag{56}$$

Note that $\phi_2(s_1) = \phi_1'(s_1)\phi_1(s_1)$ and selecting the vector $\chi = [\chi_1, \chi_2]^T = [\phi_1(s_1), s_2]^T$ and $\rho = \frac{\beta(t)}{\phi_1'(s_1)}$, it is possible to rewrite system (56) as follows:

$$\dot{\chi} = \phi_1'(s_1) \left[A\chi + B\rho \right], \tag{57}$$

where matrices A and B are defined as follows:

$$A = \begin{bmatrix} -k_1 & 1 \\ -k_2 & 0 \end{bmatrix} \quad , \quad B = \begin{bmatrix} 0 \\ 1. \end{bmatrix} \tag{58}$$

Case I - Unperturbed system: Consider the case when the approximation of $H(t)$ through $\Delta \hat{H}(t)$ is exact, i.e., $\epsilon(t) = 0$. Then, choosing the Lyapunov function candidate (LFC) as follows:

$$V = \chi^T P \chi, \tag{59}$$

where P denotes a positive definite matrix that satisfies the Lyapunov equation

$$A^T P + PA = -Q, \tag{60}$$

where Q is any given positive definite matrix, let λ_m denote the smallest eigenvalue of Q.

Note that the proposed LFC is a continuous, positive definite, and differentiable function that satisfies the following form:

$$\lambda_{min}(P) \|\chi\|_2^2 \leq V(s) \leq \lambda_{max}(P) \|\chi\|_2^2, \tag{61}$$

where $\lambda_{min}(P)$ and $\lambda_{max}(P)$ are the smallest and largest eigenvalues of P, respectively, and $\|\chi\|_2^2 = |s_1| + 2|s_1|^{\frac{3}{2}} + s_1^2 + s_2^2$ is the Euclidean norm of χ, noting that

$$|\phi(s_1)| \leq \|\zeta\|_2 \leq \frac{V^{\frac{1}{2}}(\zeta)}{\lambda_{min}^{\frac{1}{2}}(P)}.$$

The time derivative of V along the trajectories of the system leads to

$$\dot{V}(\chi) = 2\chi^T P \dot{\chi}$$
$$= \phi_1'(s_1)\chi^T \left(A^T P + PA \right) \chi$$
$$= -\phi_1'(s_1)\chi^T Q \chi$$
$$\leq -\phi_1'(s_1)\lambda_m \|\chi\|_2^2$$
$$\leq -\left[\mu_2 + \frac{\mu_1}{2|s|^{\frac{1}{2}}} \right] \lambda_m \|\chi\|^2$$
$$\leq -\lambda_m \mu_2 \|\chi\|^2 - \frac{\lambda_m \mu_1}{2} \frac{\|\chi\|^2}{|s|^{\frac{1}{2}}}$$
$$\leq -\alpha_1 V - \frac{\alpha_2}{2} \sqrt{V}$$

where

$$\alpha_1 = \frac{\mu_2 \lambda_m}{\lambda_{max}(P)} \quad ; \quad \alpha_2 = \frac{\mu_1 \lambda_m \lambda_{min}^{\frac{1}{2}}(P)}{\lambda_{max}(P)}.$$

Note that $\dot{V}$ is a continuously decreasing function, and, as we can observe in the following, we can conclude that the equilibrium point is reached in finite time.

Because the solution of its analog differential equation

$$\dot{v} = -\alpha_1 v - \alpha_2 v^{\frac{1}{2}}, \quad v(0) \geq 0 \tag{62}$$

is given by

$$v(t) = \exp(-\alpha_1 t) \left[v(0)^{\frac{1}{2}} + \frac{\alpha_2}{\alpha_1} \left[1 - \exp(\frac{\alpha_1}{2} t) \right] \right]^2 \tag{63}$$

and using the comparison principle, the solution converges to the origin, as previously stated. Finally, $s_i \to 0$ in finite time, and based on (29), it is implied that $\lim_{t \to \infty} e = 0$ and $\lim_{t \to \infty} \dot{e} = 0$.

Remark 4. *From the stability proof, one can guarantee finite-time convergence of vector $s = [s_1, s_2]^T$ to zero. Note from Equation (50) that s_1 is related to σ_i, which means that $\sigma_i \to 0$, then by Equation (29), one can deduce that $e(t) \to 0$ and $\dot{e}(t) \to 0$ as time increases.*

Remark 5. *Note that for system (57) in the absence of disturbances, the necessary and sufficient condition for convergence is that matrix A is Hurwitz. This is equivalent to conditions $k_1 > 0$ and $k_2 > 0$.*

Case II. Perturbed system: Consider the case when the approximation of the $H(t)$ term is overestimated or underestimated, i.e., the TDE error $\epsilon(t) \neq 0$. Then, the robustness of the GSTA controller minimizes the influence of this disturbance. In this case, we consider the LFC defined in (59).

Remark 6. *It is assumed that the transformed perturbation $h(t)$ satisfies the sector condition Moreno (2009), which implies that $\rho(t, \chi) = |\chi_1|\beta(t)$ satisfies $|\rho(t, \chi)| \leq L|\chi_1|$. Thus, $\omega(\rho, \chi) = -\rho^2(t, \chi) + L^2\chi^2 \geq 0$, Then, this expression can be rewritten as $\omega(\rho, \chi) = -\rho^2(t, \chi) + L^2\chi^T C^T C\chi \geq 0$ with $C = [1, 0]$.*

Remark 7. *For design reasons, it is important to note that the gain matrix A in (58) can be rewritten as*

$$A = A_0 - K_0 C_0, \tag{64}$$

where

$$A_0 = \begin{bmatrix} 0 & 1 \\ 0 & 0 \end{bmatrix}, \quad K_0 = \begin{bmatrix} k_1 \\ k_2 \end{bmatrix}, \quad C_0 = \begin{bmatrix} 1 & 0 \end{bmatrix}. \tag{65}$$

The time derivative of V along the trajectories of the system gives

$$\begin{aligned}
\dot{V} &= 2\chi^T P\dot{\chi} \\
&= \phi_1'(s_1)\left[\chi^T(A^T P + PA)\chi + \chi^T PB\rho + \rho^T B^T P\chi\right] \\
&= \phi_1'(s_1)\begin{bmatrix}\chi\\\rho\end{bmatrix}^T\begin{bmatrix}A^T P + PA & PB\\B^T P & 0\end{bmatrix}\begin{bmatrix}\chi\\\rho\end{bmatrix} \\
&\leq \phi_1'(s_1)\left\{\begin{bmatrix}\chi\\\rho\end{bmatrix}^T\begin{bmatrix}A^T P + PA & PB\\B^T P & 0\end{bmatrix}\begin{bmatrix}\chi\\\rho\end{bmatrix} + \omega(\rho, \chi)\right\} \\
&= \phi_1'(s_1)\left\{\begin{bmatrix}\chi\\\rho\end{bmatrix}^T\begin{bmatrix}A^T P + PA + L^2 C^T C & PB\\B^T P & -1\end{bmatrix}\begin{bmatrix}\chi\\\rho\end{bmatrix}\right\} \\
&= \phi_1'(s_1)\left\{\begin{bmatrix}\chi\\\rho\end{bmatrix}^T\begin{bmatrix}A^T P + PA + L^2 C^T C + \overline{\alpha}P & PB\\B^T P & -1\end{bmatrix}\begin{bmatrix}\chi\\\rho\end{bmatrix}\right\} \\
&\quad - \phi_1'(s_1)\overline{\alpha}\chi^T P\chi \\
&= \phi_1'(s_1)\left\{\begin{bmatrix}\chi\\\rho\end{bmatrix}^T\underbrace{\begin{bmatrix}\begin{array}{c|c}-C_0^T K_0^T P - PK_0 C_0 + \overline{\alpha}P & PB\\+A_0^T P + PA_0 + L^2 C^T C & \\\hline B^T P & -1\end{array}\end{bmatrix}}_{W(K_0, P|\overline{\alpha}, L)}\begin{bmatrix}\chi\\\rho\end{bmatrix}\right\} \\
&\quad - \phi_1'(s_1)\overline{\alpha}\chi^T P\chi \\
&= \phi_1'(s_1)\left\{\begin{bmatrix}\chi\\\rho\end{bmatrix}^T W(K_0, P|\overline{\alpha}, L)\begin{bmatrix}\chi\\\rho\end{bmatrix}^T - \overline{\alpha}\chi^T P\chi\right\}.
\end{aligned}$$

Assume that K_0 is selected such that $P > 0$ and $\overline{\alpha} > 0$ providing $W(K_0, P|\overline{\alpha}, L) \leq 0$. The time derivative of V can then be expressed as follows:

$$\dot{V}(\chi) \leq -\overline{\alpha}\phi_1'(s_1)\chi^T P\chi \tag{66}$$

$$= -\mu_1\frac{\overline{\alpha}}{2|s_1|^{\frac{1}{2}}}V - \mu_2\overline{\alpha}V \tag{67}$$

$$\leq -\frac{\mu_1\overline{\alpha}\lambda_{\min}^{\frac{1}{2}}(P)}{2}V^{\frac{1}{2}} - \mu_2\overline{\alpha}V. \tag{68}$$

The fact that the derivative of V is negative definite is reached by selecting positive gains k_1 and k_2 sufficiently high to satisfy the condition $W(K_0, P|\overline{\alpha}, L) \leq 0$. Therefore, it can be concluded that the equilibrium point is reached in a finite time from any initial condition.

Following the same procedure as in the previous case, the solution of the analog differential equation of (68) is given by

$$v(t) = \left[v(0)^{\frac{1}{2}} + \frac{\mu_1\lambda_{\min}^{\frac{1}{2}}(P)}{2\mu_2}\left[1 - \exp\left(\frac{\mu_2\overline{\alpha}}{2}t\right)\right]\right]^2 \cdot \tag{69}$$
$$\cdot \exp(-\mu_2\overline{\alpha}t),$$

it follows that the solution converges in finite time to the origin at the latest time T, computed as follows:

$$T = \frac{2}{\mu_2\overline{\alpha}}\ln\left(\frac{2\mu_2}{\mu_1\lambda_{\min}^{\frac{1}{2}}(P)}v(0)^{\frac{1}{2}} + 1\right). \tag{70}$$

Finally, using the comparison principle, it can be stated that $\xi_1^d(t)$ converges to $\xi_1(t)$ at latest in time given by (70).

Remark 8. *The gains of the proposed controller were selected by solving W as stated in the proof of Theorem 1. Matrix $W(K_0, P|\alpha, L) < 0$ is a bilinear matrix inequality (BMI) owing to the product of P and K_0. To solve this problem as a linear matrix inequality (LMI), the following matrix is introduced:*

$$Y = PK_0. \tag{71}$$

Matrix W can be rewritten as follows:

$$W = \left[\begin{array}{c|c} -C_0^T Y^T - YC_0 + \overline{\alpha}P & PB \\ A_0^T P + PA_0 + L^2 C^T C & \\ \hline B^T P & -1 \end{array} \right]. \tag{72}$$

This representation of W can be considered as an LMI on P and Y. Note that it is necessary to know the bound of the disturbance and a fixed positive constant value $\overline{\alpha} > 0$ to solve LMI (72) and find the the GSTA-ESO gains through the following relationship:

$$K_0 = P^{-1}Y \tag{73}$$

The TDE gains were selected based on the procedure presented in Kim et al. (2016).

Table 1
List of parameters used in simulation (values from Kim et al. (2016)).

Parameter [Units]	Symbol	Value
Rigid body mass [Kg]	m	219.8
Mass in surge [Kg]	m_u	391.5
Linear drag coefficient in surge	k_u	16
Quadratic drag coefficient in surge	$k_{u|u|}$	229.4
Mass in sway [Kg]	m_v	693.6
Linear drag coefficient in sway	k_v	131.8
Quadratic drag coefficient in sway	$k_{v|v|}$	328.3
Mass in heave [Kg]	m_w	639.6
Linear drag coefficient in heave	k_w	65.6
Quadratic drag coefficient in heave	$k_{w|w|}$	296.8
Buoyancy force in heave [N]	W	-5

Table 2
Control gains used for simulation tests.

Gain	Value
K_1	$diag(3,3,3,3)$
K_2	$diag(5,5,5,5)$
Γ	$diag(1,1,1,1)$
Δ	$diag(0.2,0.1,0.1,0.1)$
$\overline{M}$	$10 * diag(20,20,20,5)$

5. Numerical simulation results

In this section, the performance of the proposed controllers given by Equations (35) and (46) is tested under external disturbances. The objective is to demonstrate that the estimation of the dynamics of the vehicle using the TDE method improves the performance of the nominal controller, thereby reducing the chattering amplitude. The main parameters used for the simulation were obtained from the Cyclops underwater vehicle reported in Kim et al. (2016). The vehicle had a length of 1477 mm and a width of 868 mm. The parameters are summarized in Table 1 and the control gains are listed in Table 2.

Four scenarios were developed to test the performance of the proposed controllers. In the first, the vehicle followed a parameterized spiral-shaped trajectory. The sampling period was fixed to $T_s = 50\,ms$ to prove that the uncoupled controllers were independently working correctly. In the second scenario, the previous test was repeated with the sampling period increased to $T_s = 100ms$. Based on the previous test, the influence of varying the delay of the TDE on the estimation of the hydrodynamic parameters of the vehicle was indicated. In certain cases, AUVs are programmed to perform pipeline-monitoring tasks, for example, where cameras are used as sensors to measure the distance between the vehicle and pipeline to be followed. This measurement is used as a variable to maintain a constant distance during tracking. This problem inspired the fourth scenario, wherein it was proposed that the vehicle should follow a depth profile by introducing a delay of $h = 0.4\,s$ while a desired sinusoidal

trajectory was programmed in the yaw motion. Moreover, different types of disturbances were considered in all numerical simulations. First, perturbations with sinusoidal profiles were introduced in the sway and surge control, emulating an imbalance caused by ocean currents. For heave control, a constant disturbance was introduced such that a change in buoyancy occurred in the vehicle. Finally, it is important to note that in the entire set of experiments, we compared the proposed approach, namely GSTA with TDE, to the nominal design of the GSTA provided in Guerrero et al. (2018) to demonstrate the advantages of the proposed controller.

Remark 9. *The trajectory profile for this scenario was selected because it is frequently used to test the performance of 3D position controllers (x, y, z).*

5.1. Scenario 1: Nominal case

In this scenario, the sampling period was set to $T_s = 50\,ms$. The reference trajectory was a 3D spiral function given by the following expression (74):

$$\begin{bmatrix} x \\ y \\ z \end{bmatrix} = \begin{bmatrix} sin(2t) \\ cos(2t) - 1 \\ t. \end{bmatrix} \tag{74}$$

The performances of the nominal GSTA (Guerrero et al. (2018)) and proposed GSTA with TDE for trajectory tracking without considering external disturbances are displayed in Figure 2. From this figure, it can be observed that both
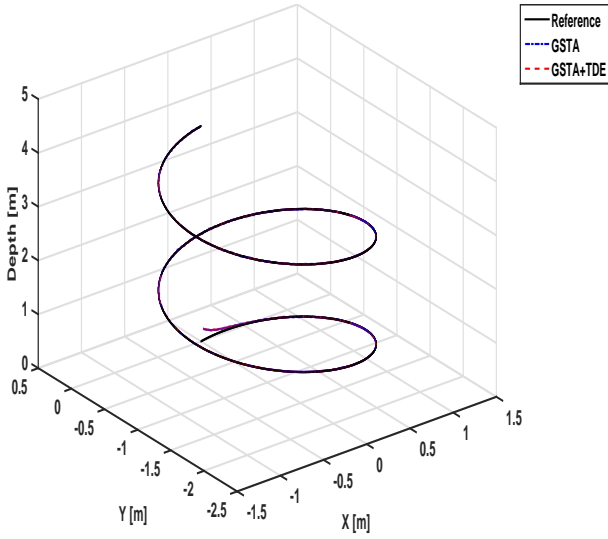
Figure 2: AUV's reference tracking of spiral-shaped path without external disturbances at sampling time of $T_s = 50\,ms$. The reference is represented by the black solid line, the nominal design GSTA (Guerrero et al. (2018)) is the solid blue line, and the solid red line is the proposed GSTA with TDE controller.

Figure 3: Underwater vehicle trajectory tracking of spiral-shaped path under external disturbances at sampling time of $T_s = 50\,ms$. The reference is represented by the black solid line, the nominal design GSTA (Guerrero et al. (2018)) is the solid blue line, and the solid red line is the proposed GSTA with TDE controller.

controllers properly followed the reference trajectory after a short period of adaptation.

The obtained results of both controllers for trajectory tracking under external disturbances are displayed in Figure 3. The disturbances in surge, sway, and heave were defined as $\rho_u = -3$, $\rho_v = 2 \times cos(2\pi f t)$, $\rho_w = -5$, and $\rho_r = 3 \times sin(2\pi f t)$ with a frequency $f = 10\,Hz$, respectively. The perturbation terms were introduced within 15 s of starting the simulation. The same disturbances were considered for all disturbed simulation scenarios. Despite the considered perturbations, the vehicle converged to the desired trajectory. It is worth noting that the GSTA controller with nominal design did not contain any information regarding the hydrodynamic parameters of the vehicle, meaning that the gain of the controller compensated for the effect of both parametric uncertainties and external disturbances. In addition, the behavior of the GSTA with TDE methodology remained close to the nominal design. Finally, it is important to note that, in general, the controllers based on sliding modes were sensitive to the sampling time; therefore, it would be interesting to consider a change in the sample time. This is discussed in the next section.

5.2. Effect of increasing the sampling period

In this test, based on the results of the study by Kim et al. Kim et al. (2016) and for a fair comparison, the sampling period of the simulations was set to $T_s = 100\,ms$. Time delay h, used to estimate the hydrodynamic parameters of the vehicle, was fixed at $h = 400\,ms$ because the DVL-provided data was at a frequency of $3\,Hz$.

The obtained results of the trajectory tracking of the vehicle considering the effects of external disturbances are displayed in Figure 4. From this figure, it can be observed that the controller with a nominal design was not capable of
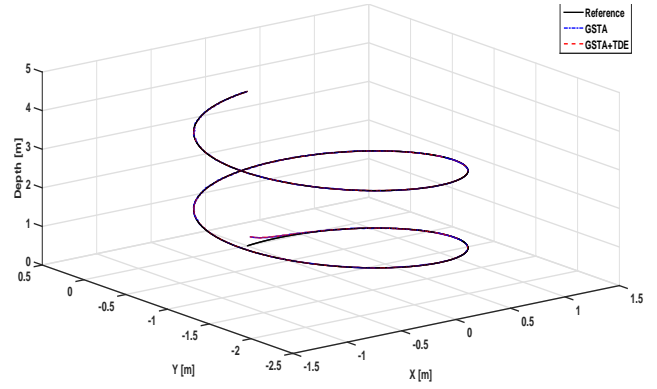
following the desired trajectory properly. Indeed, an oscillatory behavior of the vehicle around the reference trajectory can be observed, which can be explained by two arguments. First, because the hydrodynamics of the vehicle were not considered in the controller, the gain of the GSTA was required to counteract the disturbance effect. Secondly, as mentioned above, the SMC is sensitive to changes in the sampling period. To obtain superior tracking, it is mandatory to reduce the sampling time, as indicated in the results of the previous section.

The error in the tracking test of the submarine is displayed in Figure 5. As expected, the GSTA with TDE methodology significantly reduced the tracking error. The evolution of the controller input is indicated in Figure 6. These results confirm that adopting the GSTA with TDE approach can attenuate the chattering effect compared with the GSTA with a nominal design. Again, the chattering present in this simulation was due to the high sampling time.

Remark 10. *It is worth noting that the main objective of these scenarios was to demonstrate the effectiveness and robustness of the proposed method with respect to the nominal design. When the sampling period was increased, the time delay induced by the sensors also increased.*

5.3. Estimation of $H(t)$: Varying the time delay

In the previous section, it was noted that a superior estimate of $H(t)$ could be obtained if the gains of the estimator were properly tuned or the time delay of $\hat{H}(t)$ was reduced. To illustrate the influence of delay on the estimation of $H(t)$, in this simulation, the spiral trajectory was traced varying the time delay. Figure 7 displays the evolution of the trajectory tracking test with a time delay of $h = 800\,ms$. The tracking signal oscillates around the reference because of the reduction in the time delay used in the TDE for estimating matrix $H(t)$. When the time delay was reduced to $h = 200\,ms$, an upgrade in the $H(t)$ estimation was achieved,
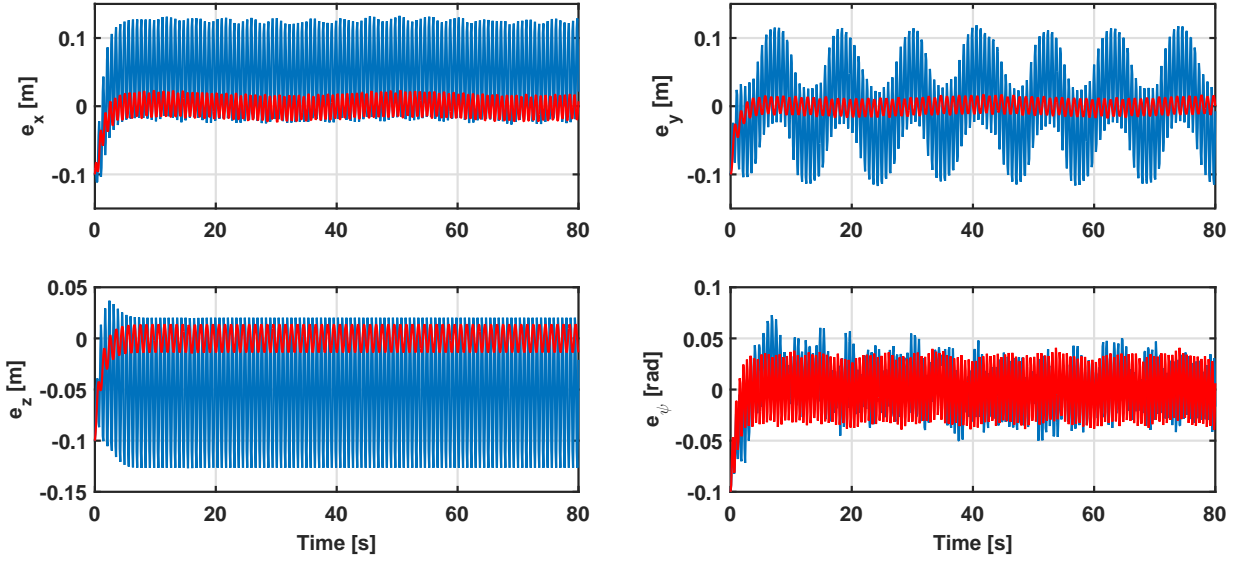
Figure 5: Robust reference tracking errors in surge (x), sway (y), heave (z), and yaw (ψ). The tracking errors were minimized by adopting the GSTA with TDE approach (solid red line) instead the GTSA nominal design represented by the solid blue line (Guerrero et al. (2018)). The sampling period was set to $T_s = 100\,ms$.
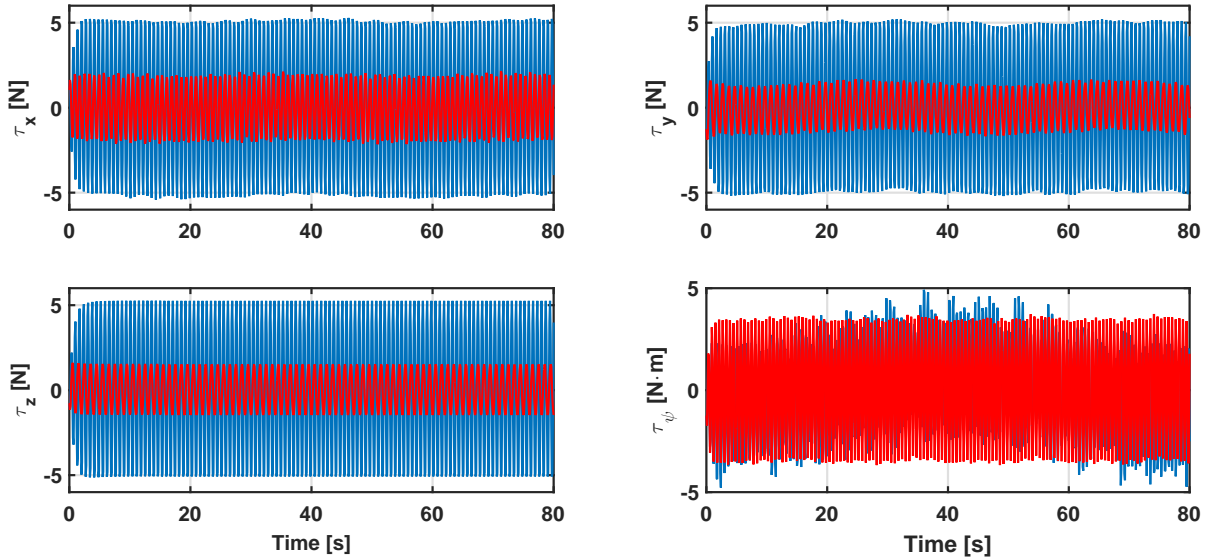

Figure 6: Control inputs for surge (u_x), sway (u_y), heave (u_z), and yaw (u_ψ) motions. The introduction of the TDE to the GSTA (solid red line) alleviates the chattering effect of the nominal design (solid blue line) Guerrero et al. (2018).

and a visible improvement in the trajectory tracking of the controller was observed (see Figure 8).

5.4. Depth and yaw trajectory tracking

Finally, the last scenario was inspired by a realistic situation, where the vehicle was programmed to perform pipeline monitoring tasks while the depth was regulated at a constant desired value. In this context, a depth profile is tracked along with a sinusoidal signal for yaw dynamics. The results for this scenario are displayed in Figure 9. By zooming around the inflection point in the depth profile, we can observe an

oscillation in the control signal due to the selected sampling period. Moreover, the tracking error increased because the depth reference function did not have a second derivative at that point. In Figure 10, yaw tracking can be observed where the same tracking effect is observed, as in the case of depth dynamics. Oscillatory behavior was clearly observed during the tracking test. However, the amplitude of the oscillations was small and did not influence the tracking task. Finally, the tracking errors of this scenario are displayed in Figure 11.
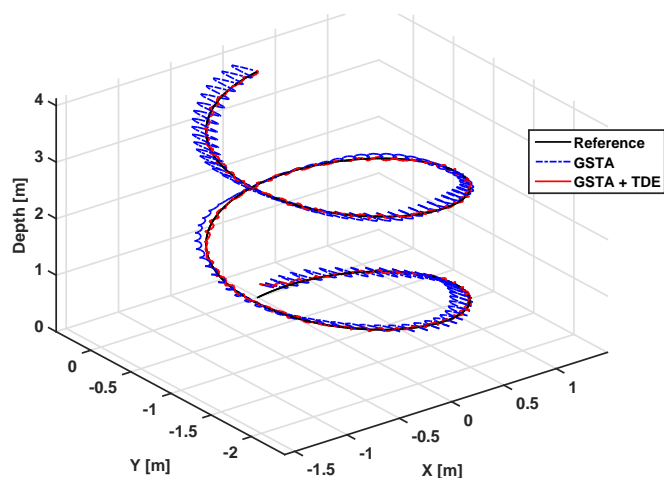
Figure 4: Underwater vehicle trajectory tracking test under persistent external disturbances at sampling time of $Ts = 100ms$. The reference is represented by the black solid line, the nominal design GSTA (Guerrero et al. (2018)) is the dashed blue line, and the solid red line is the proposed GSTA with TDE controller.
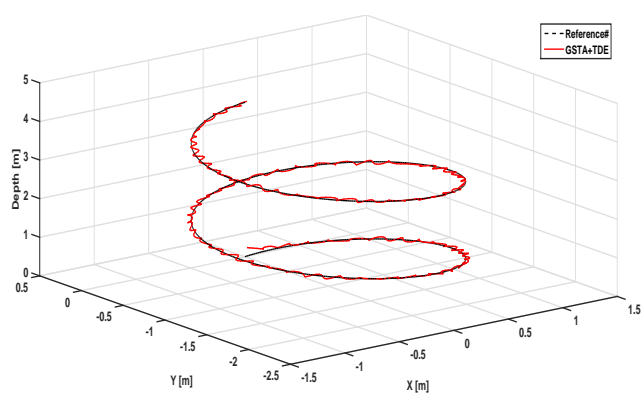

Figure 7: Effect of change of time delay on estimation of $H(t)$ for spiral tracking test when time delay is set at $h = 800\,ms$.
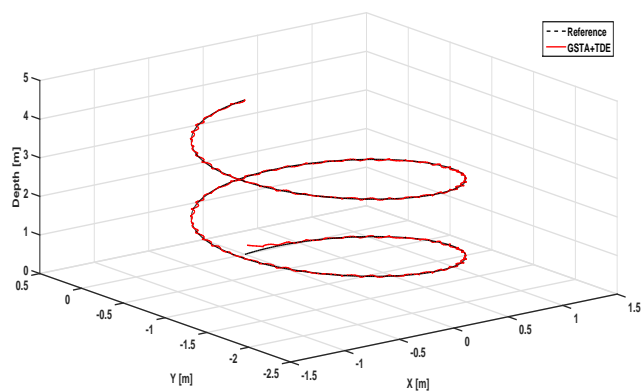

Figure 8: Effect of change of time delay on estimation of $H(t)$ for spiral tracking test when time delay is set at $h = 200\,ms$.

Remark 11. *This study was inspired by the interesting results presented in Kim et al. (2016). However, to perform a fair comparison, we decided to compare our approach*

with the GSTA nominal design, instead of comparing it with the scheme described in the cited work, where the dynamic couplings between $x - y$ and the yaw are neglected.

6. Conclusion and future work

In this study, two controllers were proposed to solve the problem of trajectory tracking of an AUV in the (x, y, z) plane and yaw dynamics. For the controller description, a nonlinear AUV model was used. The high-order sliding-mode nonlinear control technique, called the super-twisting algorithm, was improved with a TDE term. The considered TDE term estimates the vehicle hydrodynamics through time-delayed measurements, and this information is fed back to the controller to improve its performance. A stability analysis of the resulting closed-loop system was presented, and the numerical simulation results demonstrated the effectiveness and robustness of the proposed control technique. Several conditions were considered to study the influence on the system behavior, where both variations in the sampling period and time delay were considered.

A real-time implementation and validation of the proposed controller will be the subject of future research. In addition, it is should be noted that the GSTA was tested on an experimental platform; however, in the damping tests, its performance was limited because we had no method to estimate certain parameters of the vehicle model. The extension of the present results to the case of output-feedback sliding modes appears to be a challenging problem.

References

Amin, R., Khayyat, A.A., Osgouie, K.G., 2010. Neural networks control of autonomous underwater vehicle, in: Mechanical and Electronics Engineering (ICMEE), 2010 2nd International Conference on, IEEE. pp. V2–117.

Busquets, J., Busquets, J.V., Tudela, D., Pérez, F., Busquets-Carbonell, J., Barberá, A., Rodríguez, C., García, A.J., Gilabert, J., 2012. Low-cost auv based on arduino open source microcontroller board for oceanographic research applications in a collaborative long term deployment missions and suitable for combining with an usv as autonomous automatic recharging platform, in: Autonomous Underwater Vehicles (AUV), 2012 IEEE/OES, IEEE. pp. 1–10.

Caccia, M., Veruggio, G., 2000. Guidance and control of a reconfigurable unmanned underwater vehicle. Control Engineering Practice 8, 21–37.

Campos, E., Chemori, A., Creuze, V., Torres, J., Lozano, R., 2017. Saturation based nonlinear depth and yaw control of underwater vehicles with stability analysis and real-time experiments. Mechatronics 45, 49–59. doi:https://doi.org/10.1016/j.mechatronics.2017.05.004.

Campos, E. Monroy, J., Abundis, H., Chemori, A., Creuze, V., Torres, J., 2019. A nonlinear controller based on saturation functions with variable parameters to stabilize an AUV. International Journal of Naval Architecture and Ocean Engineering 11, 211–224. doi:https://doi.org/10.1016/j.ijnaoe.2018.04.002.

Chen, W., Wei, Y., Zeng, J., Han, H., Jia, X., 2016. Adaptive terminal sliding mode ndo-based control of underactuated auv in vertical plane. Discrete Dynamics in Nature and Society 2016.

Elmokadem, T., Zribi, M., Youcef-Toumi, K., 2016. Trajectory tracking sliding mode control of underactuated auvs. Nonlinear Dynamics 84, 1079–1091.

Fossen, T., . Marine Control Systems: Guidance, Navigation and Control of Ships, Rigs and Underwater Vehicles. Marine Cybernetics, Trondheim, Norway, 2002. Technical Report. ISBN 82-92356-00-2.
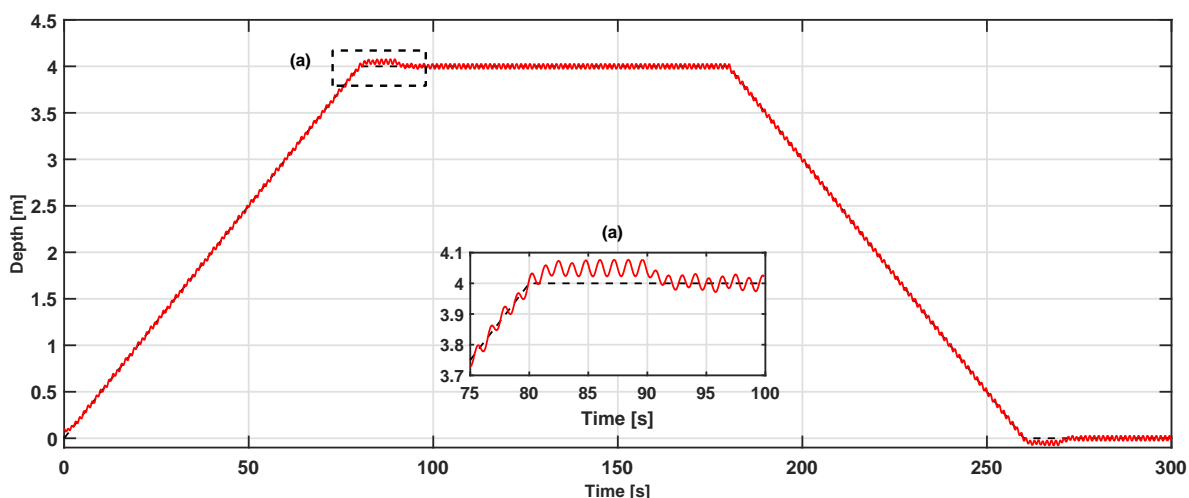
Figure 9: Robust trajectory tracking of depth profile (dashed black line) when time delay of $\hat{H}(t)$ is set at $h = 400\,ms$ and sampling time is fixed at $T_s = 100ms$. The zoomed area displays the oscillatory behavior of the GSTA with TDE approach (solid red line).

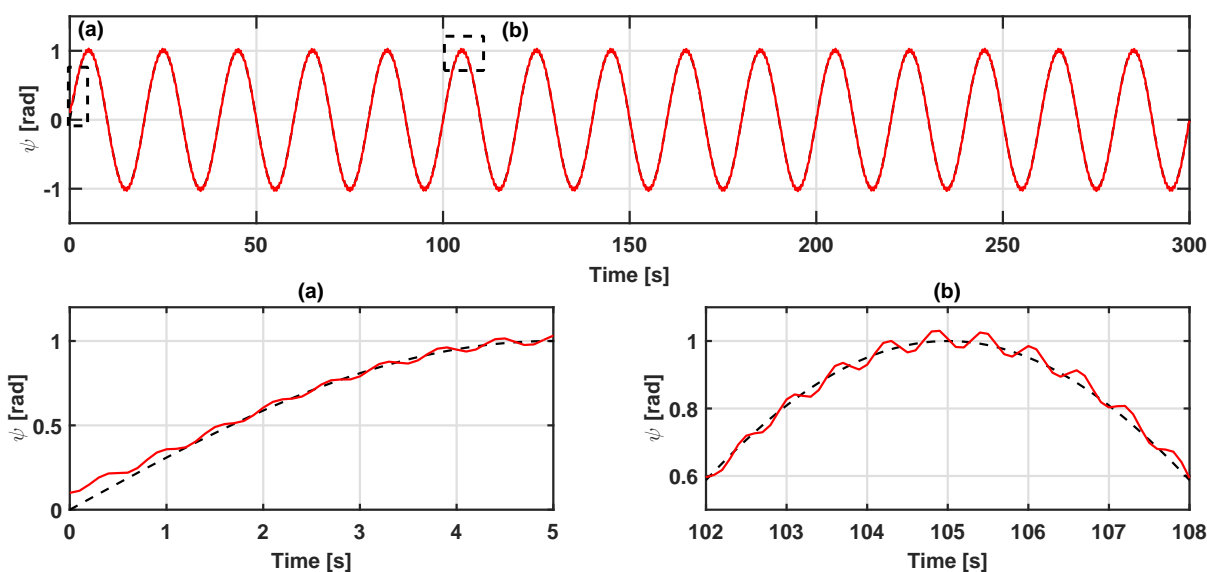**Figure 10:** Robust reference tracking for yaw dynamics when time delay of $\hat{H}(t)$ is set at $h = 400\,s$ and sampling time is set at $T_s = 100ms$. The GSTA with TDE controller (solid red line) follows the yaw reference signal (dashed black line) despite external disturbances.

Fossen, T.I., 1994. Guidance and control of ocean vehicles. John Wiley & Sons Inc.

Fridman, L., Shustin, E., Fridman, E., 1996. Steady modes and sliding modes in the relay control systems with time delay, in: Proceedings of 35th IEEE Conference on Decision and Control, IEEE. pp. 4601–4606.

Gouaisbaut, F., Dambrine, M., Richard, J., 2002. Robust control of delay systems: a sliding mode control design via lmi. Systems & Control Letters 46, 219–230. URL: https://www.sciencedirect.com/science/article/pii/S0167691101001992, doi:https://doi.org/10.1016/S0167-6911(01)00199-2.

Guerrero, J., Torres, J., Antonio, E., Campos, E., 2018. Autonomous underwater vehicle robust path tracking: Generalized super-twisting algorithm and block backstepping controllers. Journal of Control Engineering and Applied Informatics 20, 51–63.

Guerrero, J., Torres, J., Creuze, V., Chemori, A., 2019a. Trajectory tracking for autonomous underwater vehicle: An adaptive approach. Ocean

Engineering 172, 511–522. doi:https://doi.org/10.1016/j.oceaneng.2018.12.027.

Guerrero, J., Torres, J., Creuze, V., Chemori, A., 2020a. Adaptive disturbance observer for the trajectory tracking of underwater vehicles. Ocean Engineering 200, 107080. doi:https://doi.org/10.1016/j.oceaneng.2020.107080.

Guerrero, J., Torres, J., Creuze, V., Chemori, A., 2020b. Observation-based nonlinear PD control for robust trajectory tracking for autonomous underwater vehicles. IEEE Journal of Oceanic Engineering 45, 1190–1202. Https://doi.org/10.1109/JOE.2019.2924561.

Guerrero, J., Torres, J., Creuze, V., Chemori, A., Campos, E., 2019b. Saturation based nonlinear PID control for underwater vehicles: Design, stability analysis and experiments. Mechatronics 61, 96–105. doi:https://doi.org/10.1016/j.mechatronics.2019.06.006.

Hsia, T.S., 1989. A new technique for robust control of servo systems. IEEE Transactions on Industrial Electronics 36, 1–7.
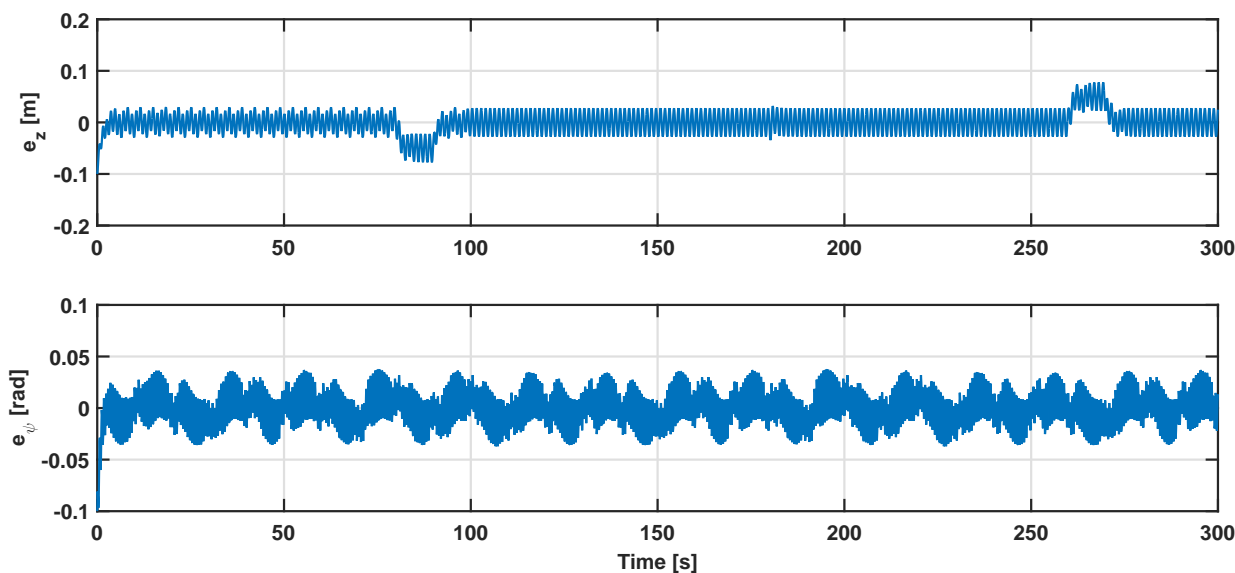
Figure 11: Trajectory tracking error evolution of depth and yaw dynamics under external disturbances.

Hsia, T.S., Lasky, T., Guo, Z., 1991a. Robust independent joint controller design for industrial robot manipulators. IEEE transactions on industrial electronics 38, 21–25.

Hsia, T.S., Lasky, T., Guo, Z., 1991b. Robust independent joint controller design for industrial robot manipulators. IEEE transactions on industrial electronics 38, 21–25.

Huang, J., Wen, C., Wang, W., Jiang, Z.P., 2013. Adaptive stabilization and tracking control of a nonholonomic mobile robot with input saturation and disturbance. Systems & Control Letters 62, 234–241.

Huang, J., Wen, C., Wang, W., Jiang, Z.P., 2014. Adaptive output feedback tracking control of a nonholonomic mobile robot. Automatica 50, 821–831.

Huang, J., Wen, C., Wang, W., Song, Y.D., 2015. Global stable tracking control of underactuated ships with input saturation. Systems & Control Letters 85, 1–7.

Jalving, B., 1994. The ndre-auv flight control system. IEEE Journal of Oceanic Engineering 19, 497–501.

Jin, M., Kang, S.H., Chang, P.H., 2008. Robust compliant motion control of robot with nonlinear friction using time-delay estimation. IEEE Transactions on Industrial Electronics 55, 258–269.

Jung, S., Hsia, T.C., Bonitz, R.G., 2004. Force tracking impedance control of robot manipulators under unknown environment. IEEE Transactions on Control Systems Technology 12, 474–483.

Kanakakis, V., Valavanis, K.P., Tsourveloudis, N., 2004. Fuzzy-logic based navigation of underwater vehicles. Journal of intelligent & robotic systems 40, 45–88.

Kim, J., Joe, H., Yu, S.c., Lee, J.S., Kim, M., 2016. Time-delay controller design for position control of autonomous underwater vehicle under disturbances. IEEE Transactions on Industrial Electronics 63, 1052–1061.

Kinsey, J.C., Eustice, R.M., Whitcomb, L.L., 2006. A survey of underwater vehicle navigation: Recent advances and new challenges, in: IFAC Conference of Manoeuvering and Control of Marine Craft.

Levant, A., 1993. Sliding order and sliding accuracy in sliding mode control. International journal of control 58, 1247–1263.

Li, J.H., Lee, P.M., 2005. A neural network adaptive controller design for free-pitch-angle diving behavior of an autonomous underwater vehicle. Robotics and Autonomous Systems 52, 132–147.

Maalouf, D., Creuze, V., Chemori, A., 2012. A novel application of multivariable l1 adaptive control: From design to real-time implementation on an underwater vehicle, in: Proc. IEEE/RSJ Int. Conf. Intel. Robots

and Systems, Algarve, Portugal.

Moreno, J.A., 2009. A linear framework for the robust stability analysis of a generalized super-twisting algorithm, in: Electrical Engineering, Computing Science and Automatic Control, CCE, 2009 6th International Conference on, IEEE. pp. 1–6.

Prestero, T., 2001. Development of a six-degree of freedom simulation model for the remus autonomous underwater vehicle, in: OCEANS, 2001. MTS/IEEE Conference and Exhibition, IEEE. pp. 450–455.

Rathore, A., Kumar, M., 2015a. Robust steering control of autonomous underwater vehicle: based on pid tuning evolutionary optimization technique. International Journal of Computer Applications 117.

Rathore, A., Kumar, M., 2015b. Robust steering control of autonomous underwater vehicle: based on pid tuning evolutionary optimization technique. International Journal of Computer Applications 117.

Rezazadegan, F., Shojaei, K., Sheikholeslam, F., Chatraei, A., 2015. A novel approach to 6-dof adaptive trajectory tracking control of an auv in the presence of parameter uncertainties. Ocean Engineering 107, 246–258.

Salgado-Jiménez, T., García-Valdovinos, L.G., Delgado-Ramírez, G., 2011. Control of rovs using a model-free 2nd-order sliding mode approach. Sliding Mode Control , 347–368.

Salgado-Jimenez, T., Jouvencel, B., 2003. Using a high order sliding modes for diving control a torpedo autonomous underwater vehicle, in: OCEANS 2003. Proceedings, IEEE. pp. 934–939.

Shen, C., Shi, Y., Buckham, B., 2018. Trajectory tracking control of an autonomous underwater vehicle using lyapunov-based model predictive control. IEEE Transactions on Industrial Electronics 65, 5796–5805.

Shtessel, Y., Edwards, C., Fridman, L., Levant, A., 2014. Sliding mode control and observation. volume 10. Springer.

Smallwood, D.A., Whitcomb, L.L., 2004. Model-based dynamic positioning of underwater robotic vehicles: Theory and experiment. IEEE Journal of Oceanic Engineering 29, 169–186.

Tabar, A.F., Azadi, M., Alesaadi, A., 2015. Sliding mode control of autonomous underwater vehicles. World Academy of Science, Engineering and Technology, International Journal of Computer, Electrical, Automation, Control and Information Engineering 8, 546–549.

Tijjani, A.S., Chemori, A., Creuze, V., 2020. Robust adaptive tracking control of underwater vehicles: Design, stability analysis and experiments. IEEE/ASME Transactions on Mechatronics 26, 897–907. doi:https://doi.org/10.1109/TMECH.2020.3012502.

Tijjani, A.S., Chemori, A., Creuze, V., 2022. A survey on tracking control of unmanned underwater vehicles: Experiments-based approach. Annual Reviews in Control doi:https://doi.org/10.1016/j.arcontrol.2022.07.001.

Utkin, V., Guldner, J., Shi, J., 2017. Sliding mode control in electromechanical systems. CRC press.